NON-LINEAR BEHAVIOUR OF A WING DUE TO UNDERWING STORES

G.A. Vio*,† , D.S. Stanley*,‡
***School of Aerospace, Mechanical and Mechatronic Engineering, The University of Sydney, Sydney NSW 2006, Australia**
†gareth.vio@sydney.edu.au; ‡dstanley@sydney.edu.au

Keywords: *Non-Linear Aeroelasticity, Wing-Store Interaction*

Abstract

Many high performance aircraft operating in the transonic regime carry multiple combinations of external stores which can alter the aeroelastic behaviour and result in dynamic instabilities. Unlike much of the previous research into wing/store behaviour, the current work investigates a combined non-linear structural and linear aerodynamic model and explores the behaviour observed.

1 Introduction

Advancements in aviation technology and design continue to produce lighter and optimised aircraft structures which makes them more likely to manifest undesirable aeroelastic phenomena. Self-sustaining oscillations, otherwise known as Limit Cycle Oscillations (LCOs), are one type of dynamic aeroelastic instabilities which are bounded in amplitude, and are caused by an interaction between aerodynamic and structural forces. Aircraft that operate in the transonic regime often carry a range of external stores on the underside of the wing, including missiles, bombs, external fuel tanks and pods. LCOs have been report to occur in flight [1] and have been encountered computationally [2, 3]. LCOs are not just restricted to wing/store configurations. Other investigations have reported the presence of non-linear behaviour in clean configuration [4].

The first systematic investigations into the effect of store aerodynamics on wing-store flutter were conducted in 1982 by Turner [5] which resolved that there were instances where neglecting store aerodynamics would lead to overestimations of flutter speed. Contemporary studies have continued to be directed towards aerodynamic models including transonic shocks or induced flow separation and have in most cases neglected nonlinear structural damping as a contributor to LCO occurrence. Mignolet et al suggests a possible method to produce an alternate coupled aero-structural model [6]. Configurations with external stores including the effect of wing sweep [7] and delta wings [8] have been studies. Abbas et al [9] determined that both the store and pylon significantly impact the dynamic aeroelastic instabilities with cantilevered wings, where geometric non-linearities have considerable impact on the overall bifurcation response when taken into account Limit Cycle Oscillations continue to arise in modern military fighter aircraft, including the F-16/E [6]. The undesirable effects of LCOs range from weapon aiming difficulties, a reduction in aircraft manoeuvrability, structural fatigue and potential structural failure to a limitation in the aircrafts flight envelope to avoid particular LCO vibration bounds. The major mechanism that causes LCOs in wing/store problems is yet to be fully understood and still poses problems in terms of modelling and understanding. By better understanding the mechanics and interaction between non-linearities, an accurate picture of the actual aeroelastic behaviour

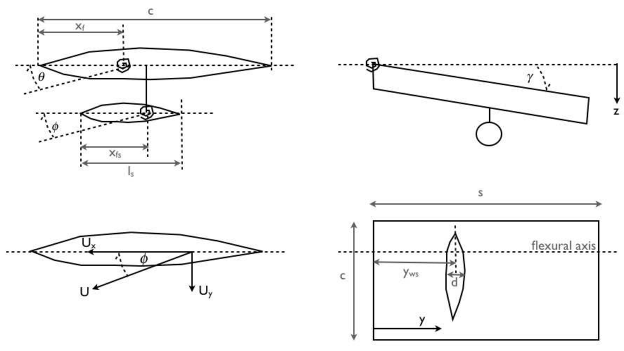

Fig. 1 Hancock model with store

due to wing/store configurations can be provided. This in turn has the potential to expand flight envelopes by having accurate safe ranges to work with, whilst also providing a cost effective solution for research planning in aircraft development and flutter testing certification [6, 10].

2 Non-Linear Aeroelastic Model

A modified version of the Hancock aeroelastic model [11] is used in this study. The Hancock model is a straight rigid rectangular wing with a bending and torsion spring at the root. The aerodynamics is modelled using strip theory. An underwing store is added and its properties are calculated using inertial coefficient for an ellipsoid [12].

The aeroelastic equation of motion can be written as

$$(A_s + A_a)\ddot{q} + (\rho V B + D)\dot{q} + (\rho V^2 C + E)q = 0 \tag{1}$$

where ρ is the air density and V is the airspeed. The subscript s and a refer to the wing structural inertia and store aerodynamic inertia respectively. The matrix A corresponds to the system's inertia, B, C are the aerodynamic damping and aerodynamic stiffness and D and E are the structural damping and stiffness matrices. q is a vector of degree of freedom of the form

$$q = \begin{bmatrix} \gamma & \theta & \alpha \end{bmatrix}^T \tag{2}$$

where γ is the bending degree-of-freedom, θ the twisting degree-of-freedom and α the store pitching degree-of-freedom, as defined in figure 1. The matrices of the whole system have the following form:

$$\begin{aligned}
A_s &= \begin{bmatrix} I^w_\gamma + I^s_\gamma & I^w_{\gamma\theta} + I^s_{\gamma\theta} & I^s_{\gamma\alpha} \\ I^w_{\gamma\theta} + I^s_{\gamma\theta} & I^w_\theta + I^s_\theta & I^s_{\theta\alpha} \\ I^s_{\gamma\alpha} & I^s_{\theta\alpha} & I^s_\alpha \end{bmatrix} \\
A_a &= -k_3' J_3 \rho \begin{bmatrix} 0 & 0 & 0 \\ 0 & 0 & 0 \\ 0 & 1 & 1 \end{bmatrix} \\
B &= \tfrac{1}{2}\rho V \begin{bmatrix} -\frac{s^3 c a_w}{3} & 0 & 0 \\ \frac{s^2 c^2 b_{1w}}{2} & M_{\dot\theta} c^3 s & 0 \\ 2y_{ws}(k_2 - k_1)vol & 0 & 0 \end{bmatrix} \\
C &= \tfrac{1}{2}\rho V^2 \begin{bmatrix} 0 & -\frac{c a_w s^2}{2} & 0 \\ 0 & c^2 b_{1w} s & 0 \\ 0 & 2(k_2 - k_1)vol & 2(k_2 - k_1)vol \end{bmatrix} \\
D &= \begin{bmatrix} C_\gamma & 0 & 0 \\ 0 & C_\theta & 0 \\ 0 & 0 & C_\alpha \end{bmatrix} \\
E &= \begin{bmatrix} K_\gamma & 0 & 0 \\ 0 & K_\theta & 0 \\ 0 & 0 & K_\alpha \end{bmatrix}
\end{aligned} \tag{3}$$

where vol is the store volume, c is the wing chord, s is the wing span, a_w is the lift coefficient, $b_{1w} = ec$ and e is defined as $\frac{x_{fw} - 1/4c}{c}$ where x_{fw} is the location of the flexural axis. The C_i and K_i term are the damping and structural stiffness terms. The store inertial terms are given by:

$$\begin{aligned}
k_1 &= \frac{\alpha_0}{2-\alpha_0} \\
k_2 &= \frac{\beta_0}{2-\beta_0} \\
k_3 &= \frac{\gamma_0}{2-\gamma_0} \\
k_1' &= \frac{(b^2-c^2)(\gamma_0-\beta_0)}{(b^2+c^2)[2(b^2-c^2)+(b^2+c^2)(\beta_0-\gamma_0)]}
\end{aligned} \tag{4}$$

where the coefficient are given by the elliptical integral

$$\begin{aligned}
\gamma_0 &= abc \int \frac{d\lambda}{(c^2+\lambda)\sqrt{(a^2+\lambda)(b^2+\lambda)(c^2+\lambda)}} \\
\gamma_0 &= \frac{2abc}{(b^2-c^2)\sqrt{a^2-c^2}} \left[\frac{b}{ac}\sqrt{a^2-c^2} - E\left\{\phi, \sqrt{\frac{a^2-b^2}{a^2-c^2}}\right\} \right] \\
\phi &= \tan^{-1}\left(\sqrt{\frac{b^2}{c^2} - 1} \right)
\end{aligned} \tag{5}$$

The θ_0 and β_0 terms can be obtained by cycling through the permutation of the store axis. The $E\{\bullet\}$ is an incomplete elliptic integral of the second kind and is evaluated using the method of arithmetic-geometric mean and descending landed transformation [13].

The structural stiffness elements are fixed as follows

$$\begin{bmatrix} K_\gamma \\ K_\theta \\ K_\alpha \end{bmatrix} = 2\pi(24.5) \begin{bmatrix} 1 \\ 1.27 \\ 0.55 \end{bmatrix} \tag{6}$$

while the damping terms are defined as proportional damping terms, with a constant of proportionality of 10^{-4} with respect to the stiffness matrix.

3 Non-Linear Stiffness and Damping

Non-linearities appear in all system and can have a significant effect on the response of a system. Here two types of non-linearities will be introduced, namely a free-play non-linearity, equation 7, and a Coulomb friction-linearity (equation 8). Typical restoring force graphs are shown in figure 2. The free-play non-linearity can be mathematically defined as

$$M(x) = \begin{cases} kx + k\delta \mathrm{sgn}(x) & |x| \geq \delta \\ 0 & |x| < \delta \end{cases} \tag{7}$$

where δ is the size of the free-play region and sgn is the signum function. The Coulomb non-linearity can be expressed as follows

$$G(\dot{x}) = c\dot{x} + \mu F_n \mathrm{sgn}(\dot{x}) \tag{8}$$

where μ is the coefficient of friction and F_n the normal force.

For this paper both non-linearities are located on the store degree-of-freedom.

4 Wing Stores

Wing stores are commonly found in a vast array of aircraft, from simple general aviation to high performance transonic regime aircraft. The purpose of these stores can be divided into the two

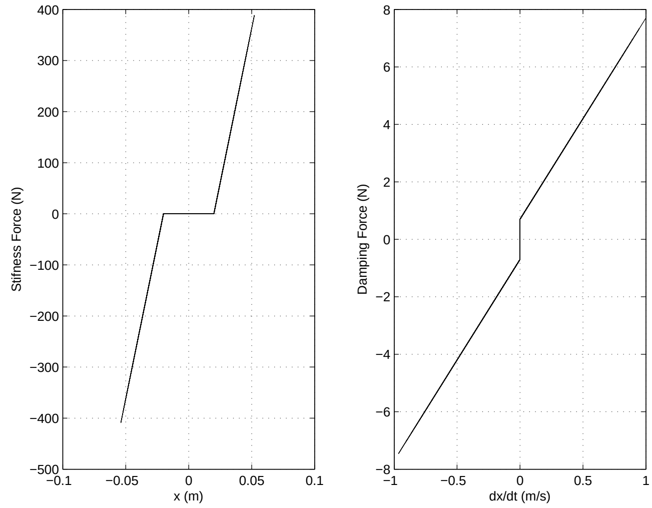

Fig. 2 Restoring Forces Diagram

categories of armament or weapon systems and external fuel storage. The effects of store aerodynamics and particularly the role of friction damping on the flutter behaviour of a wing has often been considered both too complex computationally or of little importance to the overall aircraft behaviour. However, with the developments in computational processing power we are able to develop the current wing models to incorporate wing stores that illustrate the known interactions.

4.1 Wing Store Types

Previous investigations [6, 5] have narrowed their scope of research to focus on the three main types of wing stores carried by many contemporary military aircraft as follows:

- **AIM Missles**. This air to air missile has a range of variations including the ‘Sparrow’ (AIM-7F/M/P/R), the ‘Sidewinder’ (AIM-9L/M/S/P/X), the AMRAAM (AIM-120C) and the ASRAAM (AIM-132). AIM missiles are commonly manufactured by Raytheon and are used throughout the world, but particularly in the United States. The range of these missiles is between 8 - 50 km, and have high fineness ratios between 17 - 24 [14].

- **External Fuel Tanks**. These fuel tanks usually are much wider in diameter and heavier than other types of wing stores. The F-16 has three different options for external fuel carriage, carrying two tanks of between 300 - 600 gallons (1135 - 2271 L) of fuel. The fineness ratios of fuel tanks are much lower than the AIM missile.

- **MK-84 Bombs**. This is just one variant of a range of air-to-surface weapons that can be carried by the F-16. Similar to the external fuel tanks, these stores will often be much heavier than the air-to-air weapons.

In order to implement specific store types into the aeroelastic model, the major dimensions and weights of the different store types mentioned above are required. Those used by the aeroelastic model have been listed in Table 1. Where data is from [14, 15] and fuel carriage dimensions are based on the maximum store length and back calculations using volume to determine diameters.

4.2 Equivalent F-16 model

As the aeroelastic model representing the wing has a rectangular planform, it was required to obtain an ‘equivalent’ wing in order to model the F-16 and its stores. This section discusses the approximations and assumptions of the wing and stores that were employed in the aeroelastic model in order to best replicate an F-16 aircraft.

The Hancock model presented in the previous chapter uses a rectangular wing. However the type of aircraft that would usually carry wing stores do not have a rectangular planform. As a result, the development of the equivalent wing parameters for implementation in to the aeroelastic model are required. The F-16 planform is shown in figure 3. The F-16/C dimensions are listed in Table 2.

Assuming a rectangular planform we can then obtain the wing chord $c = 2.95\ m$. The thickness of the wing ranges between 0.08 - 0.16 m at the tip and root. As the model has a uniform thickness which must remain relatively small compared with the other dimension, a thickness of $t = 0.12\ m$ was chosen, which leaves the thickness at 4% of the chord dimension. The reference

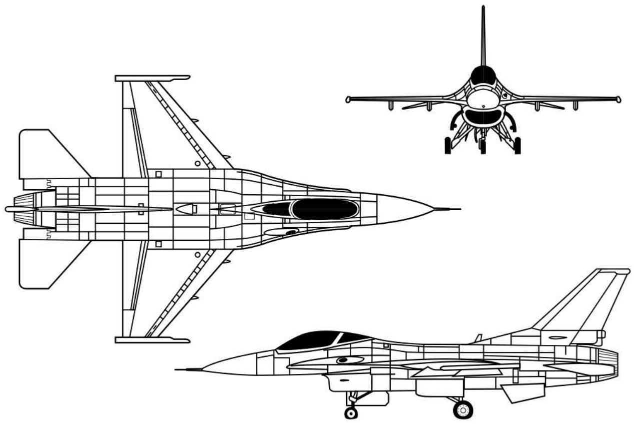

Fig. 3 The planform of an F-16 aircraft

Dimension	Value
span	9.45 m
aspect ratio	3.2
length	15.03 m
gross wing area	27.87 m^2
emplty weight	8010 kg

Table 2 F-16/C wing dimensions[16]

span is considered as the half wing and the wing weight has been approximated as 17% of the total empty weight [17], given a weight of approximately 1500 kg.

The model dimensions and operating conditions of the F-16 aircraft were benchmarked against data obtained from a test case with the aircraft configured in ‘MA 41’ mode shown in Figure 4.

This particular model configuration showed a limit cycle oscillation occurring between Mach = 0.6-1 at an altitude of 5000 ft. It was assumed that this LCO was caused by the tip missile pitch mode, the first elastic mode of the aircraft at roughly 5.6 Hz. The natural frequencies

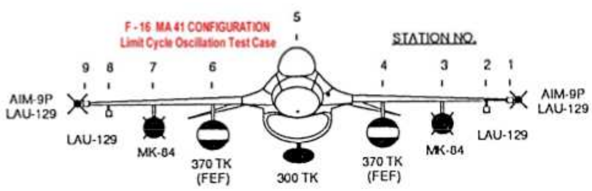

Fig. 4 MA41 Configuration of F-16 aircraft [18]

Store Type	Designation	Length (m)	Diameter (mm)	Mass (kg)	Fineness
AIM Missiles	AIM-7F	3.66	203	227	18.0
	AIM-7M/P/R	3.66	203	231	18.0
	AIM-9L/M/S	2.87	127	87	22.6
	AIM-9P	3.07	127	82	24.2
	AIM-9X	2.90	127	85	22.8
	AIM-120C	3.65	178	161	20.5
	AIM-132	2.90	166	87	17.5
Fuel Carriage	300 gallon	3.66	628	851	5.8
	370 gallon	3.66	698	1,049	5.2
	600 gallon	3.66	888	1,701	4.1
Bombs	MK-84	3.27	457	925	7.2
	MK-82	2.21	273	241	8.1

Table 1 Dimensions and Weights of Wing Stores

for the first five elastic modes for this configuration are listed in Table 3.

Mode	Frequency (Hz)
1	5.47
2	5.71
3	7.60
4	8.00
5	8.27

Table 3 Natural Frequencies of the MA41 configuration[18]

With a single AIM missile on the wingtip the natural frequencies obtained for the equivalent Hancock model are listed in table 4 and are of a similar order of magnitude obtained in the study when comparing the modes from table 3 to those in table 4 where mode 1 is bending, mode 2 is torsion and mode 3 is the mode of the store. No information was provided as to the mode sequence in [18] however, this can be considered a good correlation considering the limitations of the Hancock model.

5 Results

Non-linear simulations were run for a range of different initial conditions and store configurations as well as different airspeed. This procedure

Mode	Frequency (Hz)
1	4.02
2	9.08
3	13.90

Table 4 Natural Frequencies of single tip missile configuration

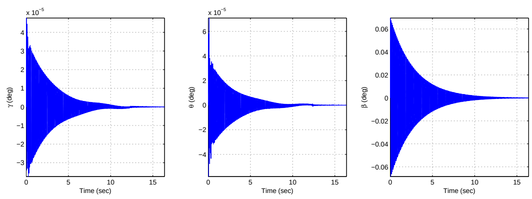

Fig. 5 Linear simulation results for half span 600 gallon fuel tank at 868 m/s

was conducted in order to determine an overview of the wing-store behaviour to provide context for the non-linear analysis.

Using the heaviest F-16 store, the 600 gallon external fuel tank with the flexural axis of the wing set to 0.4 of the store length the linear and the non-linear simulation results were compared for flight test speed of 100m/s less than the calculated flutter point, i.e. 868 m/s. The results from this test are illustrated in Figures 5 and 6.

For the same test speed, the non-linear system indicates undamped vibrations below the

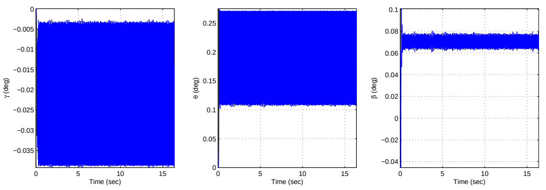

Fig. 6 Non-linear simulation results for half span 600 gallon fuel tank at 868 m/s

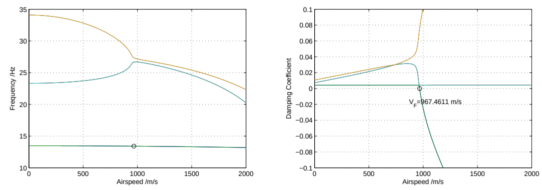

Fig. 7 v-g plot of AIM-7F missile at tip

calculated flutter speed, indicative of LCO behaviour. The linear system, as expected, displays a damped behaviour in comparison. The magnitude of the linear systems behaviour is also very small in comparison to the non-linear system. The early onset of LCOs are indicative of the suggested behaviour [6] as well as the data obtained for the F-16 specific model.

5.1 Effect of Store Types

For the stores located at the wing tip, the change in flutter speed or stability boundary was reasonably constant for different store types. The flutter speed ranged from 965.95 - 970.43 m/s for the different store types from lightest to heaviest when the store is located at the tip of the wing. Typical v-g plots are shown in figure 7.

The amplitudes of oscillation near the flutter speed for each mode were less than 1 deg. For the AIM stores, Mode 3 has a peak amplitude of 0.05 deg. Modes 1 and 2 with the AIM stores jump between the two separate equilibrium points as shown in figure 8. Mode 3 in all cases is not damped by end of the simulation, a close up of this undamped behaviour is shown in figure 9. The oscillation are inside the free-play region and do not reach the turning points, so the small amplitude LCO is due to the presence of the non-linear friction term.

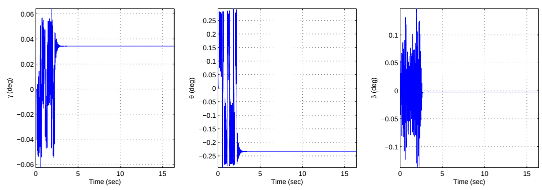

Fig. 8 Non-Linear Simulation results with AIM-7F Missile at Tip

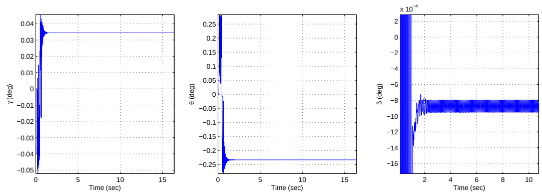

Fig. 9 Close-up o fundamped behaviour for mode 3

When locating the store at mid span the linear flutter speed ranges between 965 and 967 m/s. generally the flutter speed would reduced the closer the missile is locate to the root of the wing. The response amplitudes for stores located at half span are slightly lower than the ones located at the tip.

5.2 Effect of Airspeed

In order to determine the onset speed of particular LCOs, a range of test speeds were selected for the 370 gallon external fuel tank located at half span. Three sample results are presented in figures 10, 11 and 12. At low airspeed the response is decaying with just a static shift due to the change in equilibrium point form the free-play non-linearity. As the speed is increased a fully developed LCO is present (figure 11). As the speed is further increased the response is decaying again, showing that a non-typical LCO is present in the system.

5.3 Effect of Initial Conditions

The settling time for the store mode is greater than all the other modes. By adding an initial store displacement, the store modes response is significantly different. Not only is it much greater in magnitude, but it takes the full allotted simulation time to reach an equilibrium point. When

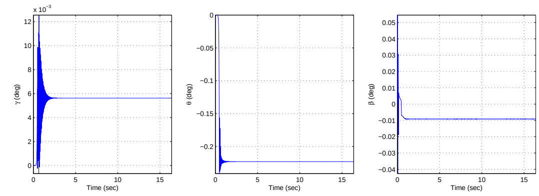

Fig. 10 Non-Linear Simulation results with 370 gallon fuel tank at half span at 400 m/s.

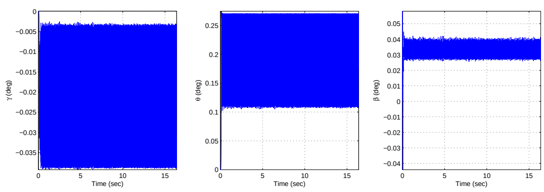

Fig. 11 Non-Linear Simulation results with 370 gallon fuel tank at half span at 868 m/s.

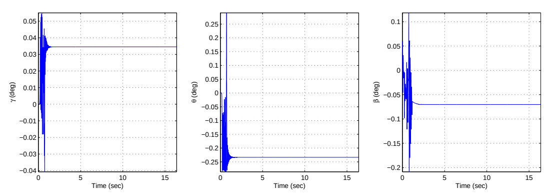

Fig. 12 Non-Linear Simulation results with 370 gallon fuel tank at half span at 968 m/s.

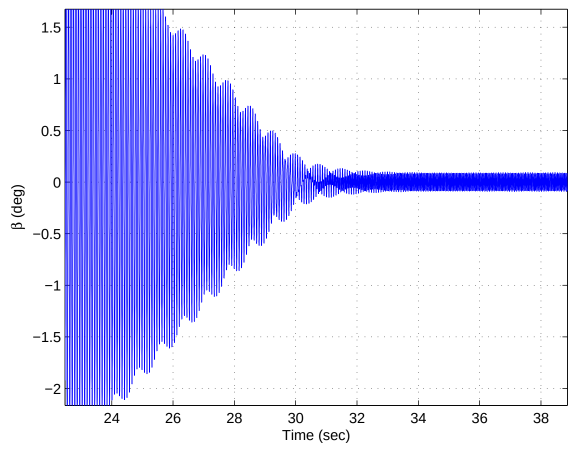

Fig. 13 Store Mode for [0 0 5 5 5 5] behaviour over longer time period

the simulation time is increased for initial conditions in the store mode has the response illustrated in figure 13. This behaviour is indicative of a limit cycle in this mode, due to this undamped response over time. When all three modes have an initial displacement the store mode has significant overshoot and once again behaves differently from the other two modes.

By doubling the size of the initial displacements, we can observe some interesting behaviours in the system response particularly in modes 2 and 3. Mode 3 has two different damping values throughout the simulation and is still significantly excited by the end of the simulation time. Mode 2 quickly reaches an undamped response in the first five seconds, then begins to reach a new equilibrium point then changing to another equilibrium point behaviour before settling to a second undamped reduced amplitude response. A close up of this behaviour can be seen in figure 14.

6 Conclusions

The appearance of Limit Cycle Oscillations in the F-16 model were found to occur at velocities below the flutter boundary points when determined from linear theory. For this reason alone it is concluded that due consideration to the effect of nonlinearities indicated throughout this paper and [6]

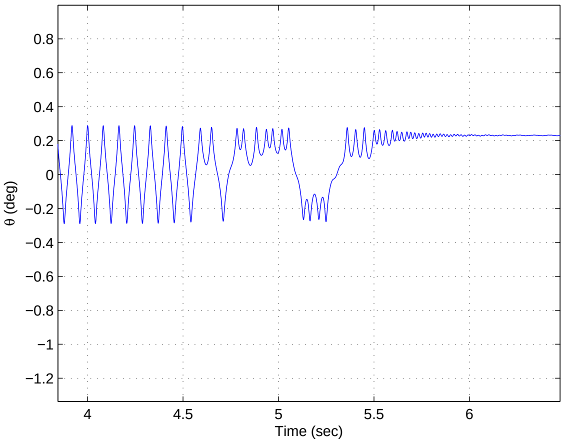

Fig. 14 Close up of system response for Mode 2 with initial conditions [0 0 0 10 10 10] at 867 m/s

continue to be considered as substantial in the aeroelastic model.

It became evident through this study that the initial conditions of the system as well as the test speeds chosen were critical in determining the specific wing/store response for a given flight envelope. Velocities either side of the utter point often contained complex behaviour, often containing high period limit cycle oscillations. The amplitudes of these LCOs often mirrored the natural frequencies of the system, however in many cases numerous dominant frequency ranges either side of these natural frequencies were present in the system response as well as the addition of harmonics.

The investigation of the non-linear behaviour of wing with store also highlights that away from bifurcation regions there are less significant changes in the systems response. This has been demonstrated through the changing of store types and the span wise location of these stores and the limited impact these changes had on the systems behaviour.

This paper has provided an enhanced overview of Limit Cycle Oscillations occurring in a wing with store as well this study has discussed the effect that parameters have on the non-linear behaviour. The derivation of an extended 3D Aeroelastic Model to include wing stores with non-linearities has shown the importance of including structural non-linearities in the analysis of the non-linear behaviour. The study has provided the necessary platform as the pre-cursor to future investigations on prediction and control of non-typical LCOs due to non-linear structural elements.

References

[1] C. M. Denegri. Limit cycle oscillation flight test results of a fighter with external stores. *Journal of Aircraft*, 37(5), 2000.

[2] G. A. Vio, G. Dimitriadis, J. E. Cooper, K. J. Badcock, M. Woodgate, and A. Rampurawala. Aeroelastic system identification using transonic CFD data for a wing/store configuration. *Aerospace Science and Technology*, 11(2-3):145–154, 2007.

[3] P. Beran, N. Khot, F. Eastep, R. Snyder, and J. Zweber. Numerical analysis of store-induced limit-cycle oscillation. *Journal of Aircraft*, 41, 2004.

[4] F. Eastep and J. Olsen. Transonic flutter analysis of a rectangular wing with conventional airfoil sections. *AIAA Journal*, 17(10):1159–1164, 1980.

[5] C. Turner. Effect of store aerodynamics on wing/store flutter. *Journal of Aircraft*, 19(7):574–580, 1982.

[6] M. Mignolet, D. Liu, and P. Chen. On the nonlinear structural damping mechanism of the wing/store limit cycle oscillation. *AIAA Journal*, pages 2148–2161, 1999.

[7] F. Gern and L. Librescu. Static and dynamic aeroelasticity of advanced aircraft wings carrying external stores. *AIAA Journal*, 36(7):1121–1129, 1998.

[8] P. Attar, E. Dowell, and D. Tang. Delta wing with store limit-cycle-oscillation modelling using a high fidelity structural model. *Journal of Aircraft*, 45, 2008.

[9] K Abbas, Q Chen, P Marzocca, and A Milanese. Non-linear aeroelastic investigations of store(s)-induced limit cycle oscillations. *Journal of Aerospace Engineering*, 222(1):63–80, 2008.

[10] G. A. Vio. *Prediction of Non-Linear Aeroelastic*

Behaviour. PhD thesis, University of Manchester, 2005.

[11] G. J Hancock, J.R. Wright, and A. Simpson. On the teaching of the principle of wing flexure-torsion flutter. *Aeronautical Journal*, pages 285–305, 1985.

[12] E. Bisplighoff, H. Ashley, and R. Halfman. *Aeroelasticity*. Addison-Wesley, 1955.

[13] M. Abramowitz and I Stegun. *Handbook of mathematical functions*. Dover, 1965.

[14] Air-Launched Missles. *Jane's All the World Aircraft*, Jan 12 2011.

[15] U.S Navy. Navy News Service - Eye on the Fleet, Nov. 26 2006.

[16] Lockheed Martin F-16 Fighting Falcon. *Jane's All the World Aircraft*, Aircraft - Fixed wing - Military, United States, Dec 23 2010.

[17] F.A. Cleveland. Size Effects in Conventional Aircraft Design. *Journal of Aircraft*, 7(6):483–512, November - December 1970.

[18] *ZAERO Application's Manual*, volume 1, chapter 2, pages 120–209. ZONA Technology Inc, 2008.

7 Copyright Statement